Int. J. Adhesion and Adhesives 17 (1997) 183–195

0143-7496/97/$17.00

PII: S0143-7496(96)00044-9

Observations of fatigue crack initiation and propagation in an epoxy adhesive

M. Dessureault and J. K. Spelt*
Department of Mechanical Engineering, University of Toronto, Toronto, Ontario, M5S 3G8 Canada
(Accepted 15 November 1996)

Fatigue crack initiation and propagation were investigated in structural adhesive joints consisting of 7075T6 aluminium adherends bonded with a mineral filled structural epoxy (Cybond 4523GB, American Cyanamid). Three types of joints were tested to achieve mode I (double-cantilever beam specimen, DCB), mixed mode I–II (cracked lap shear specimen, CLS), and mode II (end notch flexure specimen, ENF). All tests were conducted under ambient conditions with load ratio of 0.1 at a frequency of 30Hz. Fatigue loading significantly reduced the strain energy release rate (G) required to initiate a crack compared with static and quasi-static loading. For the load ranges tested, fatigue precracks doubled the time to cause a resumption of crack growth under mode I loading. Negligible differences in crack initiation times (time to generate a crack from a fillet or resume extension of an existing crack) were observed for mixed-mode I–II and mode II specimens with cracks starting from fast mode I precracks, intact fillets and fatigue precracks. For the adhesive system tested, the relative influence of the mode ratio depended on whether the rate of crack propagation was plotted versus G_{max} or $\%G_C$ (percentage of the quasi-static critical energy release rate at the particular mode ratio). When expressed as a function of $\%G_C$, debonding rates were greatest under mixed-mode conditions at a given $\%G_C$, and were indistinguishable under mode I and mode II loading. However, when expressed as a function of G_{max}, the propagation rates at a given G_{max} were the same under mixed-mode and mode I loading, and smaller under mode II loading. This means that the allowable loads for joints in fatigue will depend on the mode ratio; for mixed-mode joints it will be a smaller fraction of the quasi-static allowable load than for mode I or mode II joints. Threshold energy release rates (G_{max}) under mode I and mixed mode I–II loading were essentially the same, and were obtained equally from extrapolated crack propagation rates or crack initiation times. For this adhesive system, it is recommended that adhesive joint design be based on threshold values for zero crack growth, because crack propagation rates show too much scatter to be relied upon for the prediction of in-service subcritical crack growth, particularly under mode I and mode II loading. © 1997 Elsevier Science Ltd

(Keywords: A. epoxides; B. aluminium and alloys; C. fracture mechanics; D. fatigue)

INTRODUCTION

A fracture mechanics approach, largely based on analytical beam theory, has recently been developed for predicting the strength of adhesive joints under quasi-static load[1,2]. However, in order to develop a comprehensive methodology for predicting the strength of adhesive joints, it is necessary to consider all possible loading conditions. The objective of this research was to extend the approach used to predict quasi-static fracture loads to cases of cyclic loading.

An investigation was made to determine if a relationship exists between the quasi-static critical strain energy release rate, G_c, and the fatigue threshold strain energy release rate, G_{th}, for adhesive joints made of aluminium adherends bonded with a mineral-filled structural epoxy. Fatigue crack initiation and propagation, and threshold strain energy release rates were examined as a function of mode ratio and different crack starting conditions.

Fracture envelope

Assuming that the joint fails within the adhesive and not in the adherends, it has been shown by Fernlund *et al.*[2] that the quasi-static fracture of a wide variety of joints can be described using the fracture envelope of the adhesive system; i.e. the critical strain energy release rate, G_c, as a function of the phase angle, ψ, a parameter denoting the relative amount of mode I and mode II loading. The fracture envelope is a characteristic of the adhesive system and not the joint geometry.

Knowing the joint geometry and the applied loads, one can calculate G and ψ. If G_c of the adhesive system is known as a function of ψ, the quasi-static fracture load can then be predicted. For the general adhesive

*To whom correspondence should be addressed

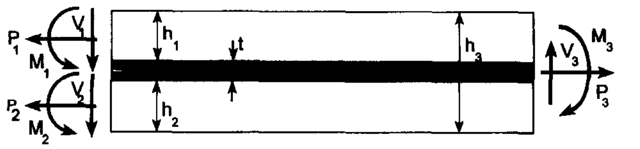

Figure 1 Cracked adhesive sandwich (analogous to a cracked homogeneous beam) where $t \ll h_1$ and h_2

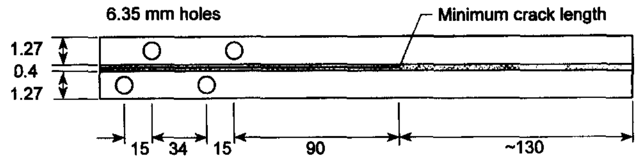

Figure 2 DCB for mode I tests — location of loading pin holes

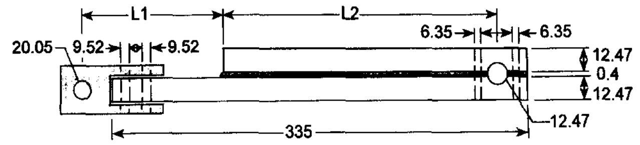

Figure 3 Typical CLS geometry. L_1 is the length from the centre of the clevis hole to the crack tip, and L_2 is the length between the crack tip and the centre of the loading pin

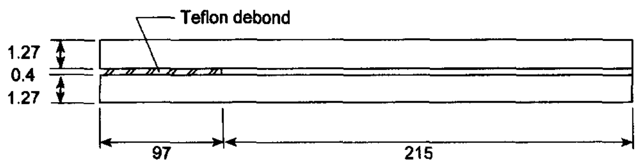

Figure 4 ENF geometry for mode II tests

joint section shown in *Figure 1*, the energy release rate is given by

$$G = \frac{P_1^2}{2E_1h_1} + \frac{M_1^2}{2E_1I_1} + \frac{P_2^2}{2E_2h_2} + \frac{M_2^2}{2E_2I_2} - \frac{P_3^2}{2E_3h_3} - \frac{M_3^2}{2E_3I_3} \tag{1}$$

where P_i is the nominal force per unit width acting on the i^{th} cross-sectional centroid at the crack tip, M_i is the nominal i^{th} moment per unit width, I_i is the second moment of area per unit width, E_i is the modulus of elasticity, and h_i is the beam thickness (since the adhesive thickness, t, is very much less than the adherend thicknesses, it is neglected in the beam thickness measurement). The phase angle, ψ, is defined as

$$\psi = atan\sqrt{\frac{G_{II}}{G_I}} \tag{2}$$

where G_I and G_{II} are the mode I and mode II components, respectively, of the applied G. Using a load jig designed by Fernlund and Spelt[3], G_c can be found conveniently for a variety of mode ratios between 0° (pure mode I) and 90° (pure mode II).

This fracture mechanics approach was used to analyze the fatigue data obtained in the following experiments.

EXPERIMENTAL

Materials and joint preparation

Three different types of joints were tested, yielding data at three mode ratios: double cantilever beam (DCB) joints for mode I, cracked-lap shear (CLS) joints for mixed mode I–II (ψ~60°), and end-notch flexure (ENF) joints for mode II. The joints were made with AA7076-T6 aluminium plates which were degreased using an FPL-etch (ASTM D2651-79, Method G). The plates were bonded with Cybond 4523GB (American Cyanamid), a mineral-filled structural epoxy adhesive. Teflon inserts were used to achieve a uniform bondline thickness of 0.4mm. The bonded plates were cured in a preheated 150°C oven for 2.5 hours at atmospheric pressure. After curing, 20-mm wide joint specimens were cut from each batch of bonded plates using a table saw (the Teflon spacers were cut away at this stage). Diluted white typing correction fluid was applied to the bondline of each specimen to aid in crack visibility. Appropriate holes and fixtures were added to the specimens prior to loading. The final three joint configurations and their dimensions are shown in *Figures 2–4*.

The quasi-static critical strain energy release rates for Cybond 4523GB at mode ratios of 0°, 60°, and 90° were, respectively, 206, 484 and 706J/m^2.

Starting conditions

Crack growth initiation was investigated as a function of two different starting conditions: intact fillet (or simulated fillet) and mode I fast precrack. The resumption of crack growth was also studied after the establishment of a fatigue precrack (pre-cycled at loads greater than or less than testing loads). This gave three levels of crack-tip sharpness; i.e. the fillet produced the smallest stress concentration and the fatigue pre-crack produced the sharpest crack tip.

The adhesive spew fillet created in the manufacture of the CLS joints was used as the intact fillet starting condition in the case of the CLS joints. A simulated adhesive fillet in the DCB and ENF joints was achieved through the use of a smooth Teflon strip inserted within the bondline during the bonding process. A mode I fast pre-crack was created by an impact blow on a chisel inserted into the bondline of the joints at the loading end. The nominal length of the precrack was controlled by placing the specimen in a vice so that the crack could only extend up to the area in compression. The fatigue precracks were made by sinusoidally loading the specimens at a constant load range for a nominal 10mm crack extension. These fatigue starting conditions resulted from previous fatigue testing; for example, a 70%P_f (where P_f is the predicted quasi-static fracture load) test was used as the starting condition for some of the 65%P_f tests. The maximum load, P_{max}, applied during testing is represented as a $\%P_f$. Note that, for the mode I (DCB) specimens, P_f was the bending moment predicted to fracture the joint under quasi-static loads. In all cases, the quasi-static fracture loads were predicted based on the location of the crack tip at the start of the test using the method of ref. 2.

Testing equipment and parameters

All tests were run sinusoidally at constant-amplitude load levels in tension with a load ratio, R of 0.1 and a frequency of 30Hz. Load cell output was monitored during each test by an oscilloscope. Testing was conducted in ambient air at a temperature of 24±2°C. Relative humidity was not controlled during testing; however, specimens were kept in a desiccator prior to testing. *Table 1* summarizes the testing parameters. The loading configurations are shown in *Figure 5*. Note that the DCB and ENF tests are loaded such that bending moments are independent of the crack length resulting in constant G tests.

A microscope was used to measure the crack length at intervals during the fatigue testing. The crack tip was taken as being the furthest visible microcrack ahead of the unobstructed crack opening (or the first visible microcrack from an intact fillet starting condition). The resolutions of the measurements were 0.02mm, 0.01mm, and 0.07mm for the DCB, CLS, and ENF joints, respectively. These resulted from the different microscope set-ups used to measure the crack length; namely, using reference marks on the side of a DCB, using a micrometer microscope mount, and using a video monitor display.

When the crack tip became difficult to distinguish, red dye penetrant was injected into the crack opening, and was given time to penetrate into the crack. After a few minutes, a new crack length measurement was taken. The crack was extended a minimum of 10mm

Table 1 Testing parameters summary

Frequency	30Hz (sinusoidal)
Environment	ambient laboratory air (temperature, 24±2°C)
Load ratio	0.1
Load type	constant-amplitude load level
Modes	1. pure mode I ($\psi=0°$) 2. mixed mode I–II ($\psi\sim60°$) 3. pure mode II($\psi=90°$)
Load levels (max. load)	1. ($\psi=0°$) 45%, 55%, 60%, 65%, and 70% of predicted quasi-static failure load 2. ($\psi\sim60°$) 35%, 40%, 45%, 55%, 60%, and 65% of predicted quasi-static failure load 3. ($\psi=90°$) 41%, 55%, and 69% of predicted quasi-static failure load
Starting conditions	1. intact fillet (no load history) 2. mode I fast pre-crack 3. previously cycled at current testing load level but loads readjusted for present crack length (CLS tests only) 4. previously cycled at a higher or lower load level

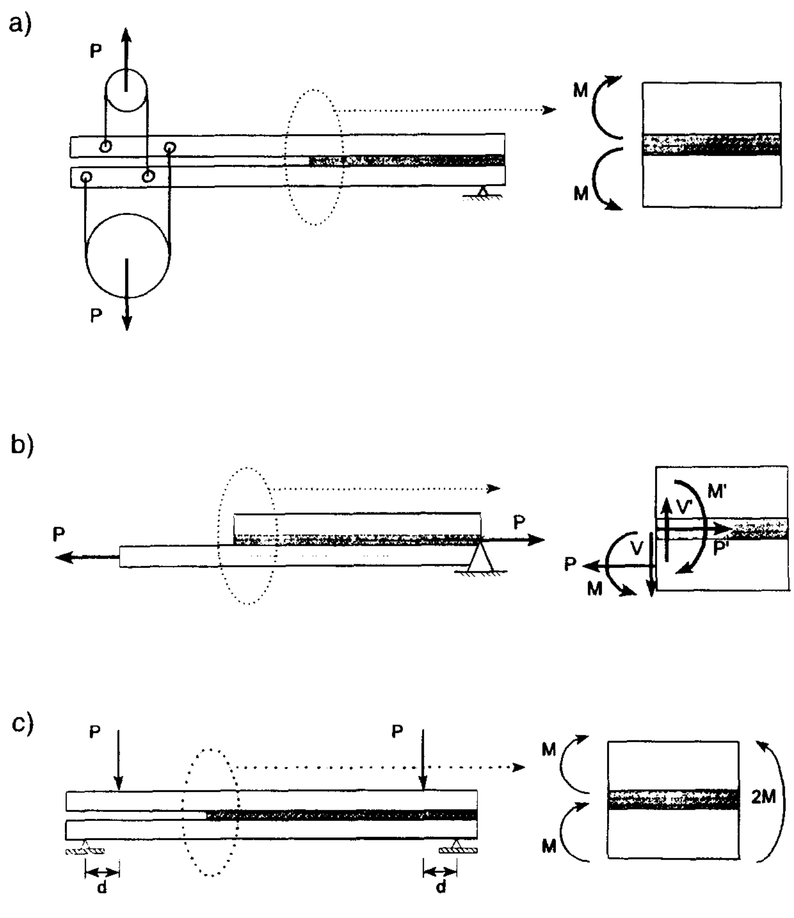

Figure 5 Loading configurations: (a) Mode I (DCB), (b) Mixed mode I–II (CLS) and (c) Mode 2 (ENF)

for tests which lasted less than 10^6 cycles. Shorter extensions were achieved for those tests which extended beyond 10^6 cycles.

The effect of the dye penetrant on fatigue crack growth behavior was investigated with the DCB and CLS tests. After obtaining several crack extension measurements, penetrant was injected into the crack and allowed to soak up to 24 h in the unloaded joint. Testing was then resumed and several more crack extension measurements were taken. Since similar crack growth rates were observed before and after the 24 hour soaking time, it was concluded that the dye penetrant as well as complete load removal had negligible effect on fatigue crack growth behaviour during the duration of a test. To verify that the intermittent cycling between observations did not affect the fatigue crack growth behaviour, the time interval between fatigue cycle sets and the duration of the cycle sets were varied. Since da/dN did not vary in a consistent way, it was assumed that the intermittent nature of the loading had a negligible effect on crack behaviour in the adhesive system used.

RESULTS AND DISCUSSION

A representative graph of measured crack length versus number of loading cycles is shown in *Figure 6*. Crack initiation time was defined as the number of cycles to the first observed crack extension. The propagation rate was obtained by performing a linear regression on the crack growth data.

Crack initiation

Mode I. The wire rope and pulley arrangement shown in *Figure 5*(a), provided a means of testing standard DCB joints so that the strain energy release rate was independent of crack length. The joint response to the applied sinusoidal loading was verified with strain gages mounted on the upper and lower adherend surfaces. An oscilloscope revealed that the strains were acceptably sinusoidal but had slightly flattened peaks and valleys which was attributed to the dynamic response of the load train.

The site for crack initiation in mode I loading was found to be highly variable. For any starting condition with an existing crack, either the crack would extend or a new microcrack would form ahead or parallel to it. However, in the case of the Teflon insert, which provided a starting condition without any prior load history, the crack initiation site was located at either the upper or lower corner of the Teflon insert. It should be noted that there was a very small amount of adhesive trapped between the Teflon and the adherends.

Under mode I cyclic loading at a given load level, it took more cycles to cause a resumption of crack growth from a pre-existing fatigue crack than it did to initiate a crack from a Teflon insert or to initiate growth from a fast mode I precrack. The load range used to create the existing fatigue cracks could be greater or less than the testing load range. The effect of a fatigue precrack can be seen in *Figure 7*, which depicts the data collected from a single DCB specimen (AA2). Test 1 was cycled at $40\%P_f$ from a fast mode I precrack for 10^5 cycles. The relatively low number of cycles at $40\%P_f$ produced no extension of the precrack prior to test 2. Test 2 (effectively beginning from a fast mode I precrack) and test 5 (precrack) were then tested at $P_{max} = 60\%P_f$. After the crack had extended approximately 10mm, P_{max} was reduced to $45\%P_f$ for a minimum of 10^6 cycles ($\sim 3.5\times10^6$ cycles for test 3, 2×10^6 cycles for test 6), after which the load was returned to $60\%P_f$. Note that throughout testing, the frequency of loading was maintained at 30Hz and R was kept at 0.1. Although the crack propagated at $60\%P_f$ from a fast mode I precrack in tests 2 and 5, it

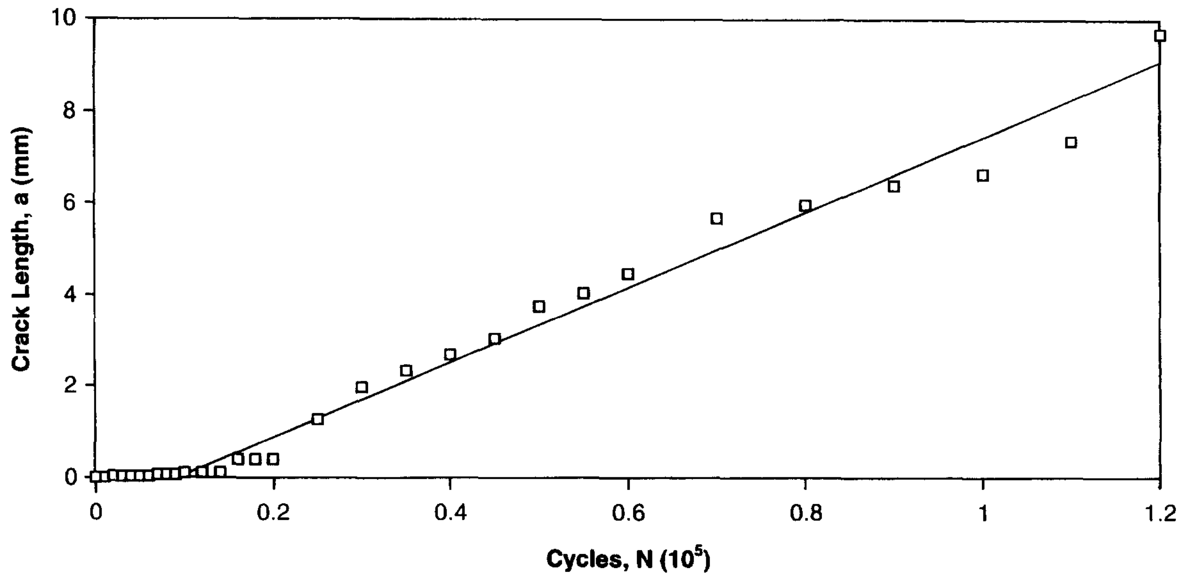

Figure 6 Representative crack growth data. The solid line represents a linear regression fit through the crack growth data points

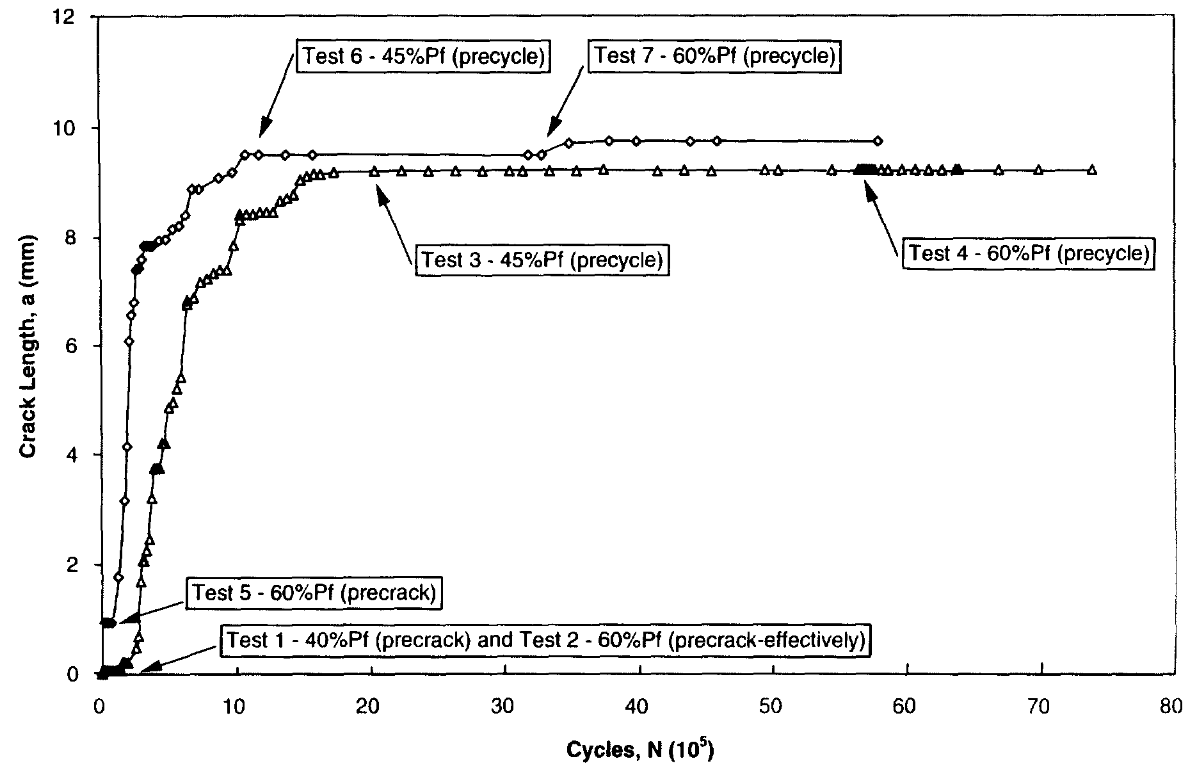

Figure 7 Example of crack growth trend of a DCB joint (specimen AA2) under various mode I fatigue loading ranges beginning from three different starting conditions. The arrows point to the start of each test

did not propagate at $60\%P_f$ from a pre-cycled fatigue crack in tests 4 and 7. It is further noted that, at $45\%P_f$, it was possible to obtain crack initiation and propagation with another DCB specimen (AA3) from a fast mode I precrack starting condition. Therefore, the $45\%P_f$ tests 3 and 6 on joint AA2, pre-cycled at $60\%P_f$, also show the effect of pre-cycling since they did not initiate cracks within 10^5 cycles. These trends suggest a blunting of the crack tip, or possibly that there is a self-toughening mechanism similar to that seen in creep crack growth tests[5].

Looking at the average time to initiation, t_i, obtained from different starting conditions, there is a consistent pattern at different load ranges (*Figure 8*). For the three load ranges with fast mode I precrack and pre-cycle starting conditions ($36\%G_c$, $42\%G_c$ and $49\%G_c$ where G_c is the quasi-static critical energy release rate for that mode ratio), the pre-cycle t_i (time to resume crack growth) is approximately twice as long as the precrack t_i. Teflon inserts appear to result in t_i which are between those for pre-cycled (greater t_i) and precracked (smaller t_i) starting conditions.

Mixed mode I–II. Starting from an intact fillet with mode ratio, ψ, of approximately 60°, the crack initiated in the fillet such that it passed by the embedded edge of the lap end at a 45° angle as shown in *Figure 9*(a), propagating towards the strap adherend. Out of 12 tests, there were three exceptions to this when the spew fillet appeared to be not well bonded at the edges [*Figure 9*(b)] and the crack initiated at the weak fillet toe. There were three out of twelve cases with CLS joints where cracks were visible at the lap end corner but not at the round surface of the fillet until further fatigue cycling.

Across the width of the CLS fillet the crack was not straight, but rather appeared jagged and stepped as if there was a damage region consisting of a succession of micro-cracks as shown in *Figure 9*(c). Then the series of short 'surface' cracks linked to form the crack front which extended into the fillet at 45° until it reached the maximum stress zone along the lap adherend surface (while still remaining in the adhesive layer).

Unlike the mode I result, no starting condition under mixed mode I–II loading consistently gave longer or shorter initiation times. This can best be seen by considering the average t_i for each starting condition at different load ranges as shown in *Figure 10* (t_i is defined as the time to the first discernible crack extension). The results suggest that the self-toughening mechanism (due to prior cyclic loading) possibly seen in mode I is effectively not present at this phase angle ($\psi \sim 60°$). It is interesting that the initiation time from a fillet was approximately the same as that from the two precracked conditions. This suggests that in-service damage would not adversely affect the fatigue performance of the bonded joint.

Mode II. The preferred crack path in mode II loading was along the upper adherend surface (for the joint orientation shown in *Figure 7*) which was subjected to compressive bending stresses. Thus, from any starting condition, the crack propagated towards the upper adherend surface while always remaining in the adhesive (cohesive failure). For the tests starting

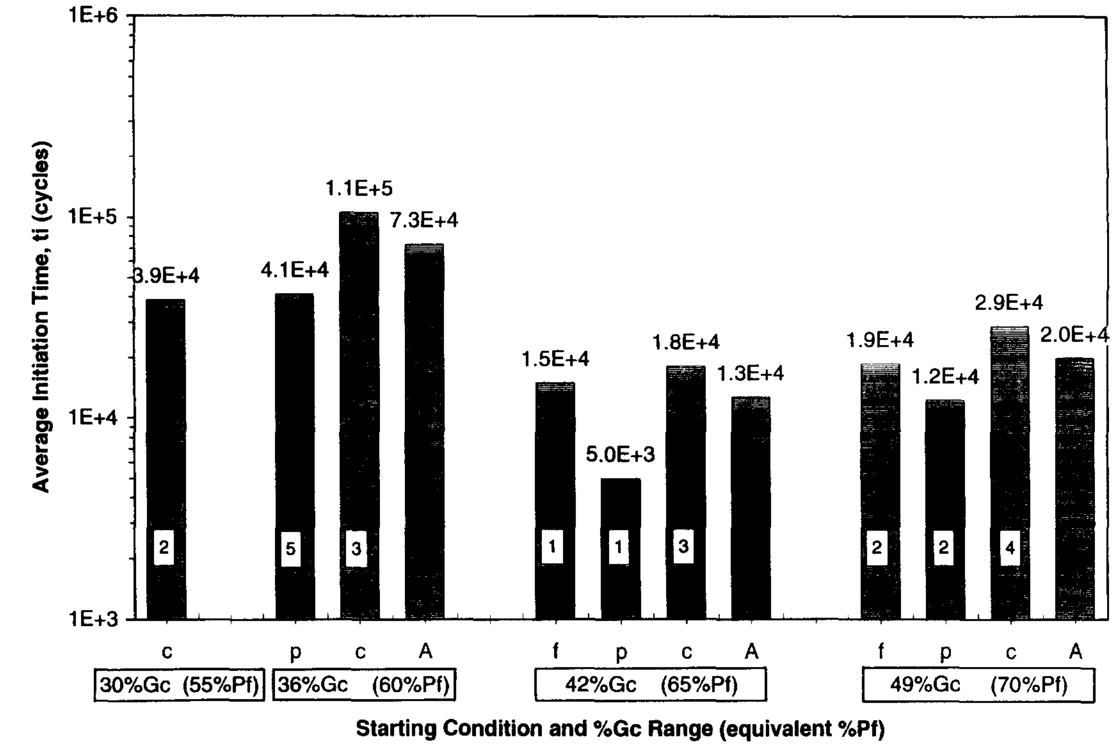

Figure 8 Mode I average initiation times for different starting conditions with t_i defined as the time to the first discernible crack extension. The time values are indicated above each column. The number appearing in the boxes within the columns corresponds to the number of data points used in averaging. Symbols for starting conditions: f — Teflon insert; p — fast mode-I precrack; c — pre-cycled at an equal or lower load; A — average of all starting conditions

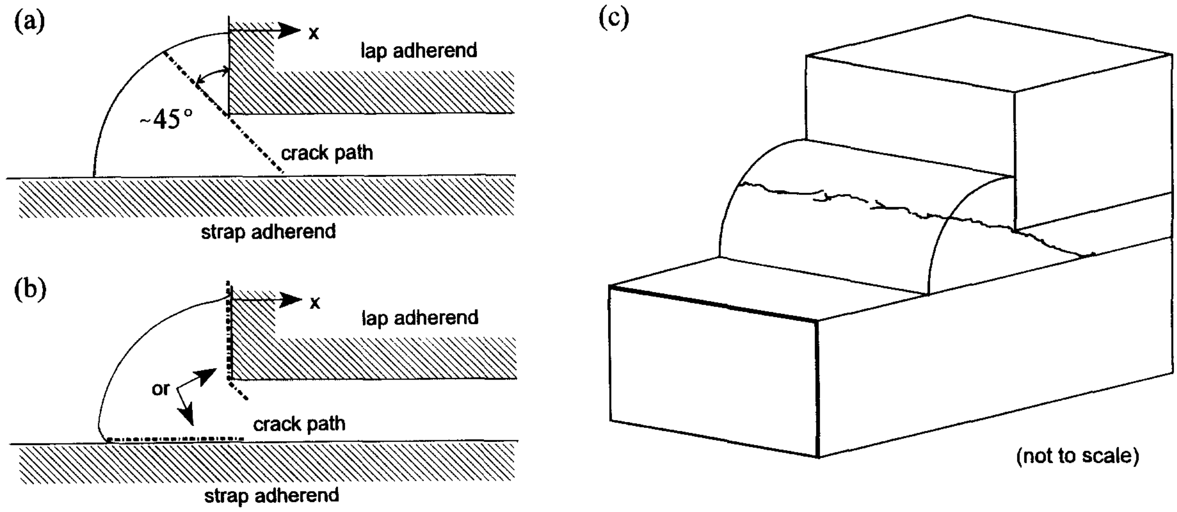

Figure 9 CLS typical fatigue crack initiation site (a), and two uncommon sites (b). (c) Typical appearance of an initiated crack through a fillet of a CLS joint. The length of the first discernible crack could be any point along the crack path shown on the side surface depending on the number of cycles elapsed before a measurement was taken

from a Teflon insert, the crack always initiated at the upper insert edge. Crack growth initiation from an existing crack (fast mode I or fatigue pre-crack) began at or very near to the existing crack tip.

Only a limited amount of initiation testing was done under mode II conditions. Based on ten tests, the data (not shown) suggest that there may be an increase in t_i if the starting condition is a pre-cycled one, as was seen in mode I. As with the other mode ratios, however, there was considerable scatter.

As expected, increasing the range of the cyclic load applied to a joint decreased the time to initiation. The relationship between load range (expressed as G_{max}) and initiation time (first discernible crack extension) is summarised for all mode ratios and starting conditions in *Figure 11*. A G_{max} asymptote exists below which a crack will not initiate; for example, $50 J/m^2$ could be taken as the asymptote in *Figure 11*. This point would be the fatigue threshold strain energy release rate, G_{th}. The data appear to lie on a single curve, suggesting

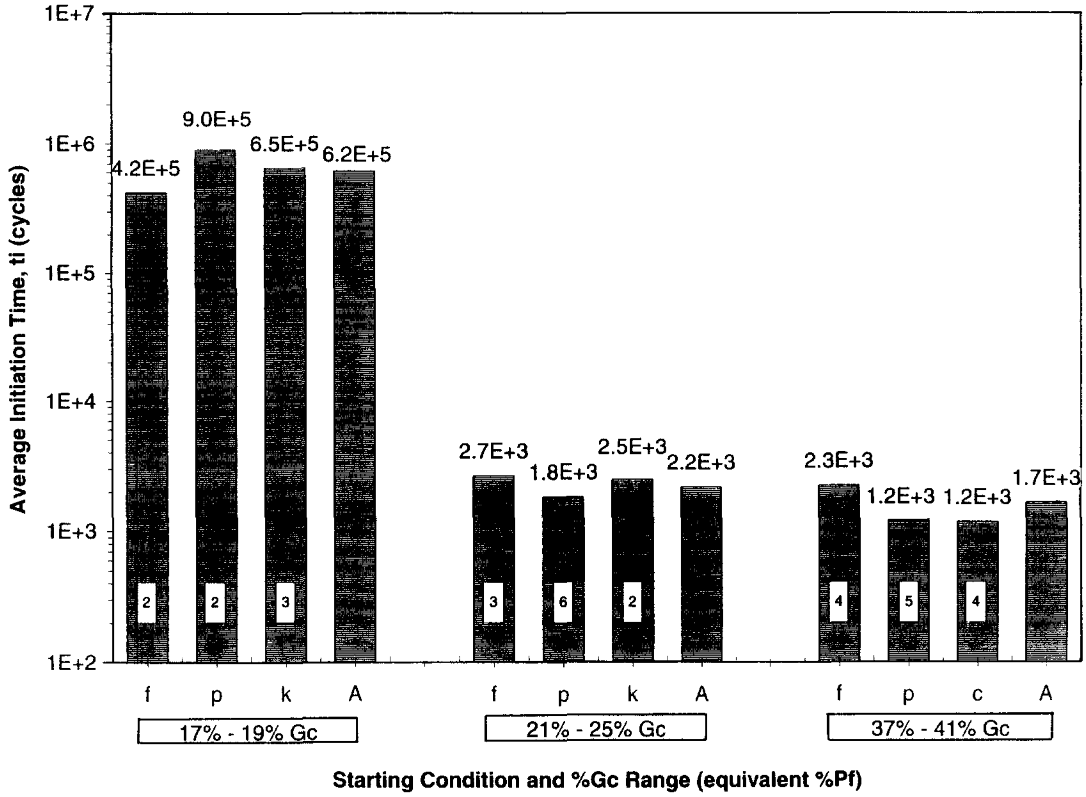

Figure 10 Effect of starting condition on mixed mode I–II fatigue initiation times — average experimental values. The time values are indicated above each column. The number appearing within the columns corresponds to the number of data points used in calculating the average. Symbols for starting conditions: f — adhesive fillet; p — fast mode I precrack; k — pre-cycled at 15% higher load; c — pre-cycled at an equal or lower load; A average of all starting conditions

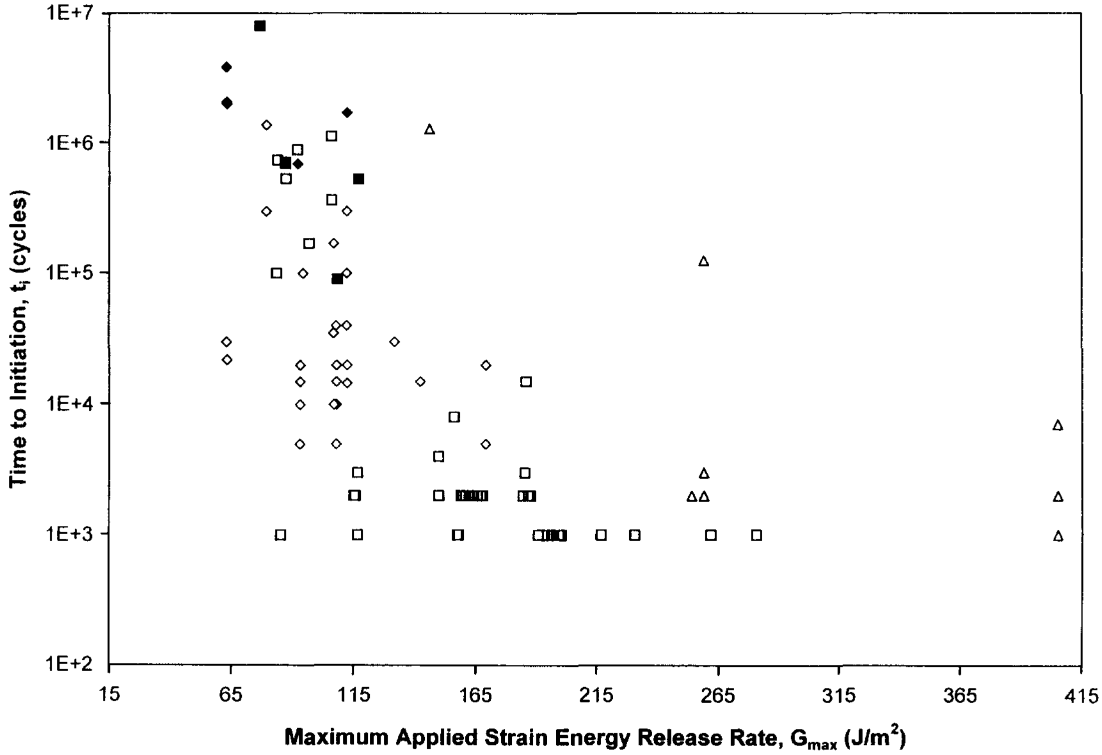

Figure 11 Fatigue crack initiation times for three mode ratios. Data points correspond to the three types of starting condition. □ mixed-mode I–II, ■ mixed-mode I–II no initiation, ◇ mode I, ◆ mode I no initiation, △ mode II

that t_i versus G_{max} is largely unaffected by the mode ratio.

Crack propagation

Crack growth behaviour in mode I, mixed mode I–II, and mode II. For the three mode ratios tested, crack propagation occurred cohesively within the adhesive. For quasi-static loading of adhesive joints, cracks have been observed to propagate in the area of the bondline with the highest mode I component of G. In the case of a DCB joint under mode I loading, the centre-line of the adhesive bondline corresponds to the maximum G location[3]. Under mode I cyclic loading, the crack propagated in a staggered, random manner (*Figure 12*) across the centre of the bondline. As with initiation, cracks could extend continuously in a jagged fashion, or new microcracks could form and propagate. These series of random extensions eventually joined up and formed a continuous crack as shown in *Figure 12*(c). Though fatigue crack growth was not as smooth as quasi-static crack growth[6], the crack path location was similar.

In CLS joints, the quasi-static crack path and the maximum G have been reported to be along the strap adherend[3,4]. Cyclic loading of CLS joints also propagated cracks along the strap adherend.

Crack growth in ENF joints ($\psi = 90°$) was also found to be limited to an area close to one particular adherend. For the loading configuration used [*Figure 5*(c)], the fatigue cracks propagated along the upper adherend only.

Propagation of a crack through the adhesive fillet in CLS joints was very quick. Many cycles may have elapsed before a crack was detected, but once it had

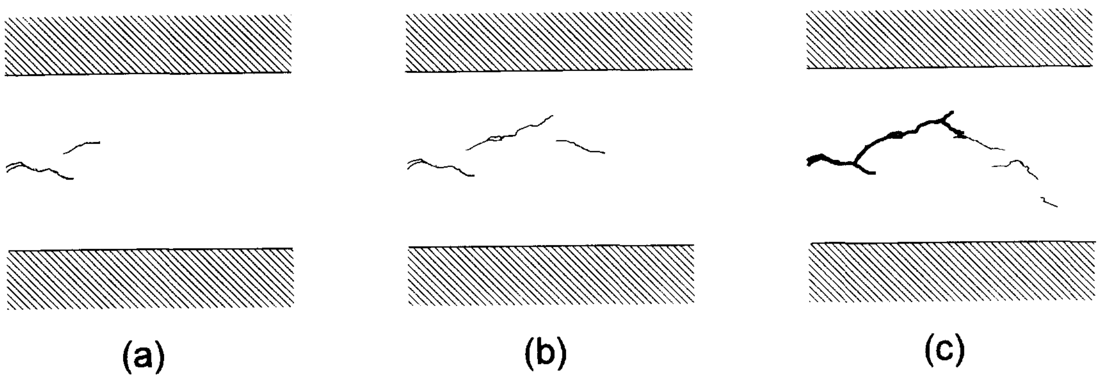

Figure 12 Typical crack propagation observed in mode I fatigue testing. From (a) to (b): stepped crack extension observed, (c) shows joining up of separate cracks into one continuous crack with more stepped extensions formed

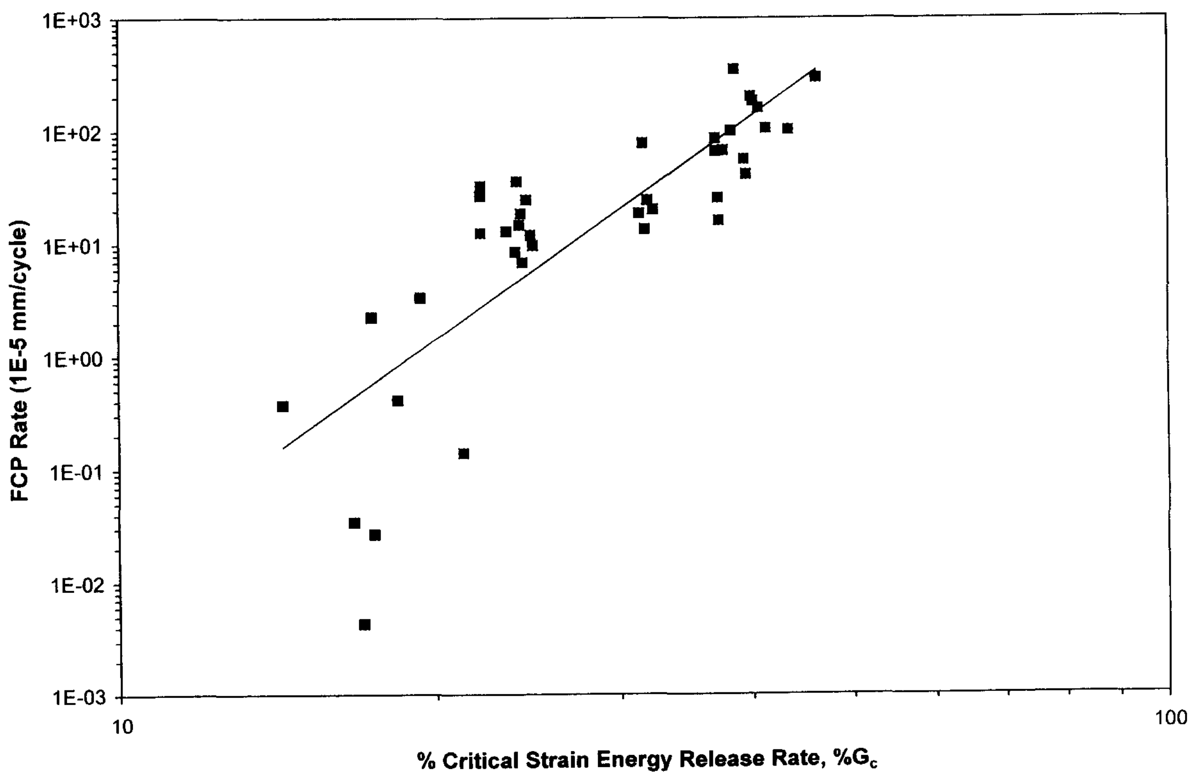

Figure 13 Fatigue crack propagation rate as a function of $\%G_C$ for mixed mode I–II tests. Regression line: $y = 4.11\text{E}{-}09x^{6.56}$ ($r^2 = 0.67$)

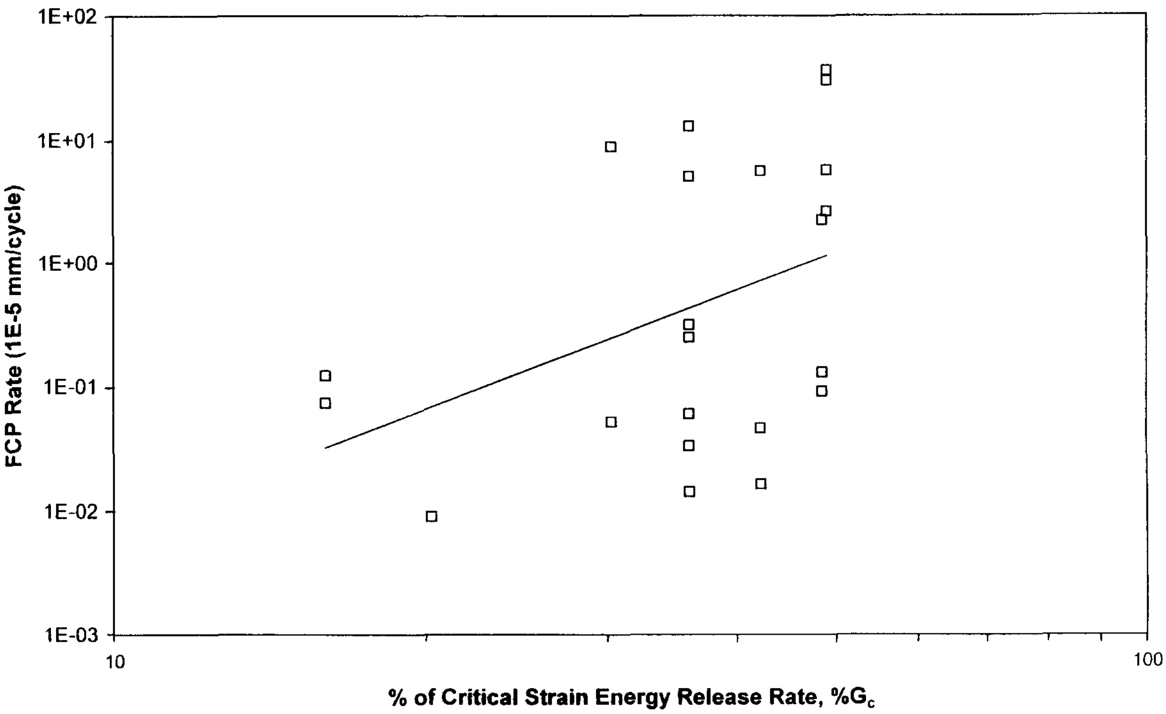

Figure 14 Fatigue crack propagation rate as a function of $\%G_C$ for mode I tests. Regression line: $y = 4.82E{-}06x^{3.18}$ ($r^2 = 0.16$)

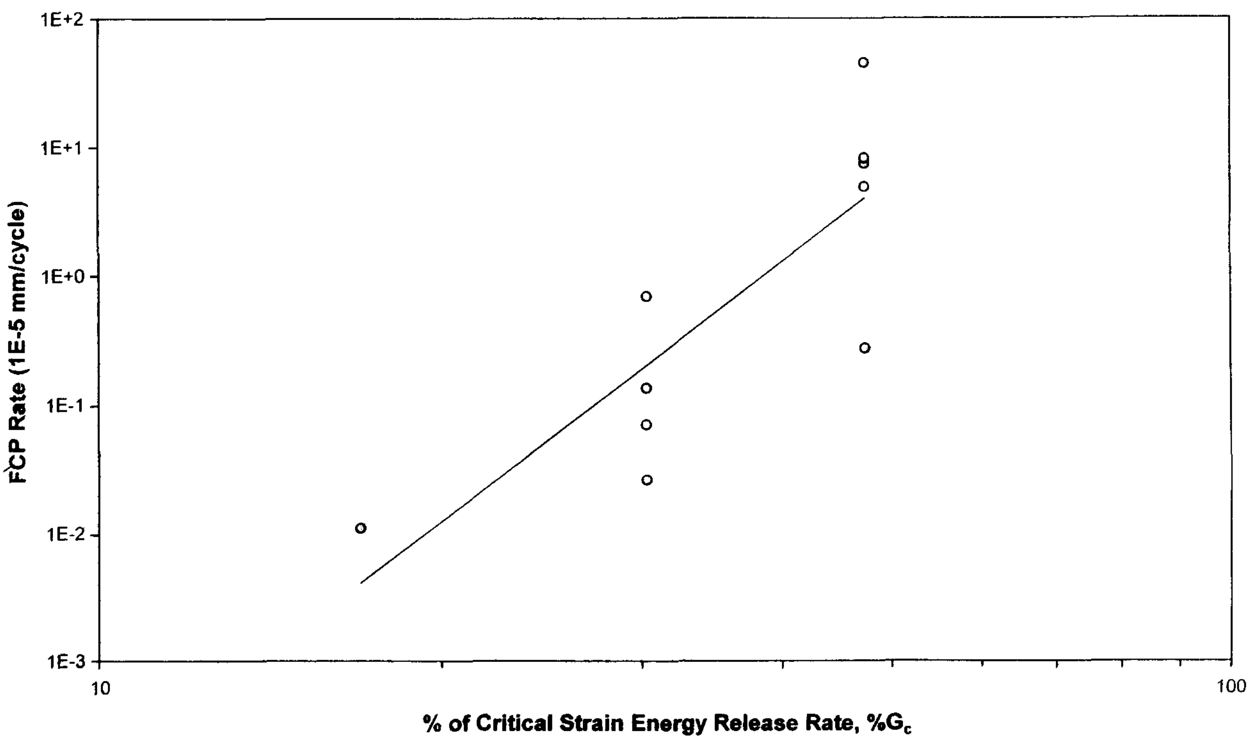

Figure 15 Fatigue crack propagation rate as a function of $\%G_c$ for mode II tests. Regression line: $y = 2.42E{-}11x^{6.69}$ ($r^2 = 0.68$)

been detected, the crack tip had usually already extended through the fillet and was located within the adhesive bondline. This was the case even if subsequent crack growth was very slow.

Figures 13–15 show the measured fatigue crack propagation rates as a function of $\%G_c$ (percentage of the quasi-static critical energy release rate for the particular mode ratio) for tests under mixed-mode I–II, mode I, and mode II, respectively.

Effect of $\%G_c$ on fatigue crack propagation rates. As expected, fatigue crack propagation (FCP) rates increased as the load range was increased for a given mode ratio. The relationship between da/dN and $\%G_c$ was linear for most of the load ranges tested and can be described by the Paris power law as

$$\frac{da}{dN} = C(\%G_c)^m \tag{3}$$

where C and m are empirical constants which are functions of material properties, loading frequency, waveform, environment, temperature, and load ratio. In this case, $\%G_c$ corresponds to the maximum applied G in fatigue testing normalized with respect to the quasi-static G_c at the mode ratio tested.

Mode ratio effect on crack growth rates. Figure 16 shows the fatigue crack propagation rate data for the three mode ratios as a function of $\%G_c$ (note that G_c varies with the mode ratio). Due to the scatter in the data, there is no clear distinction between mode I and mode II propagation behaviour. Mixed-mode results, however, are distinct, revealing significantly higher growth rates at a given $\%G_c$. In other words, cyclic loading under the mixed mode ratio was more damaging than under pure mode I or II conditions, when compared relative to the quasi-static critical energy release rate. Thus, a design rule for cyclic loading based on some allowable fraction of the quasi-static fracture strength should not use the same fraction for all mode ratios.

Figure 17 displays the data of *Figure 16* against G_{max}, the maximum strain energy release rate during a test. When compared on this basis, the mixed-mode data and the mode I data lie on a single curve which is above the mode II data. Thus, relative to G_{max}, there is no distinction between fatigue crack propagation behaviour under mixed-mode and pure mode I loading. Propagation is, however, significantly slower for a given G_{max} under pure mode 11 conditions. The trend for the combined mixed-mode and mode I data suggests a threshold energy release rate of approximately $50 mJ/m^2$, in agreement with that obtained from *Figure 11* using the time to initiation.

Although pure mode I cyclic loading caused propagation, it is interesting to note that the crack propagation rate decreased significantly during nine out of 19 tests after a certain crack extension, arresting in two of those tests. In contrast to this mode I propagation behaviour, cracks generally propagated in a constant stable manner over a 10mm crack extension under mixed mode I–II and mode II loading. The deceleration of cracks during mode I growth at constant G may be due to the self-toughening mechanism which was observed during the initiation tests and during creep crack growth[5,7].

To further establish that the difference in FCP rates for a given $\%G_c$ was indeed due to changes in mode ratio and not due to specimen variability, four previously tested CLS joints (mixed-mode I–II specimens) were converted to DCB joints by cutting off the overlap and tested under mode I cyclic loads. The mode I FCP rates obtained were consistently lower than the ones obtained under mixed mode I–II loading conditions, further confirming that the mode ratio does indeed affect FCP rates when compared on this basis.

Fatigue thresholds. Fatigue thresholds can be estimated in two ways: (a) measuring the $\%G_c$ or G_{max} at an arbitrary crack growth rate; or (b) determining the $\%G_c$ or G_{max} at which a certain number of cycles can be achieved without the initiation of a crack. The data of *Figure 16* can be used to estimate that the

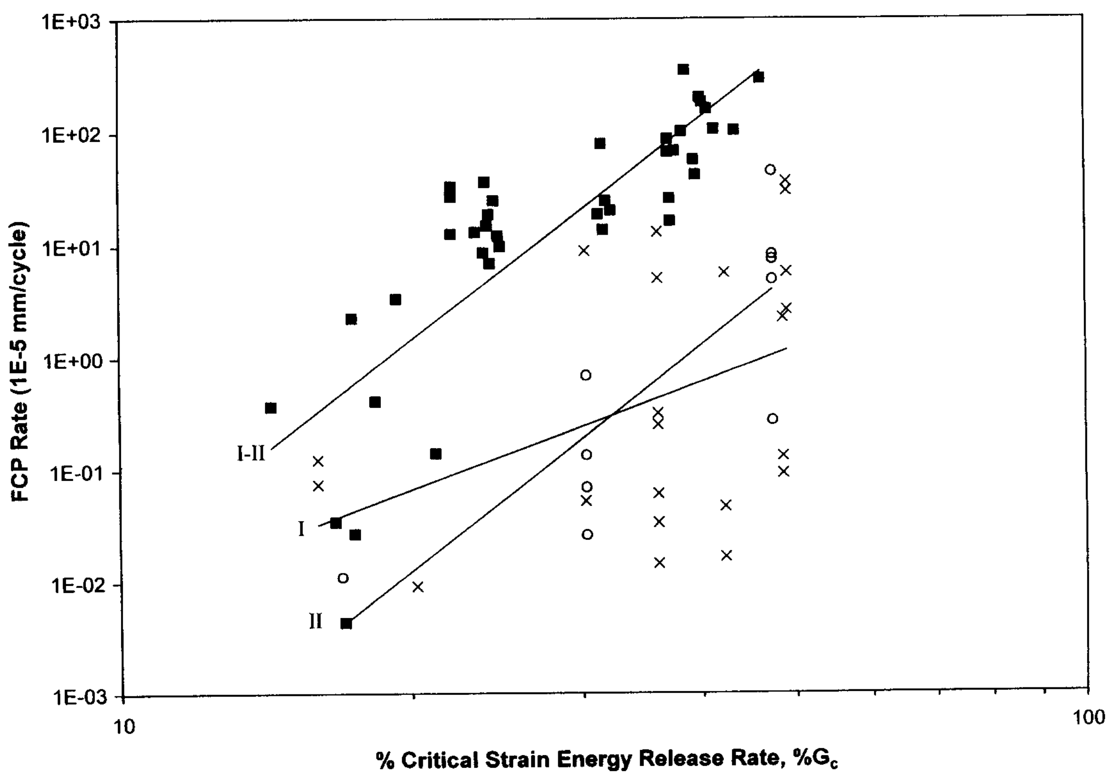

Figure 16 Fatigue crack propagation rate as a function of $\%G_c$ for tests at three mode ratios; pure mode I (X), pure mode II (○) and mixed-mode I–II (■). Linear regressions through the data are those from *Figures 13–15*

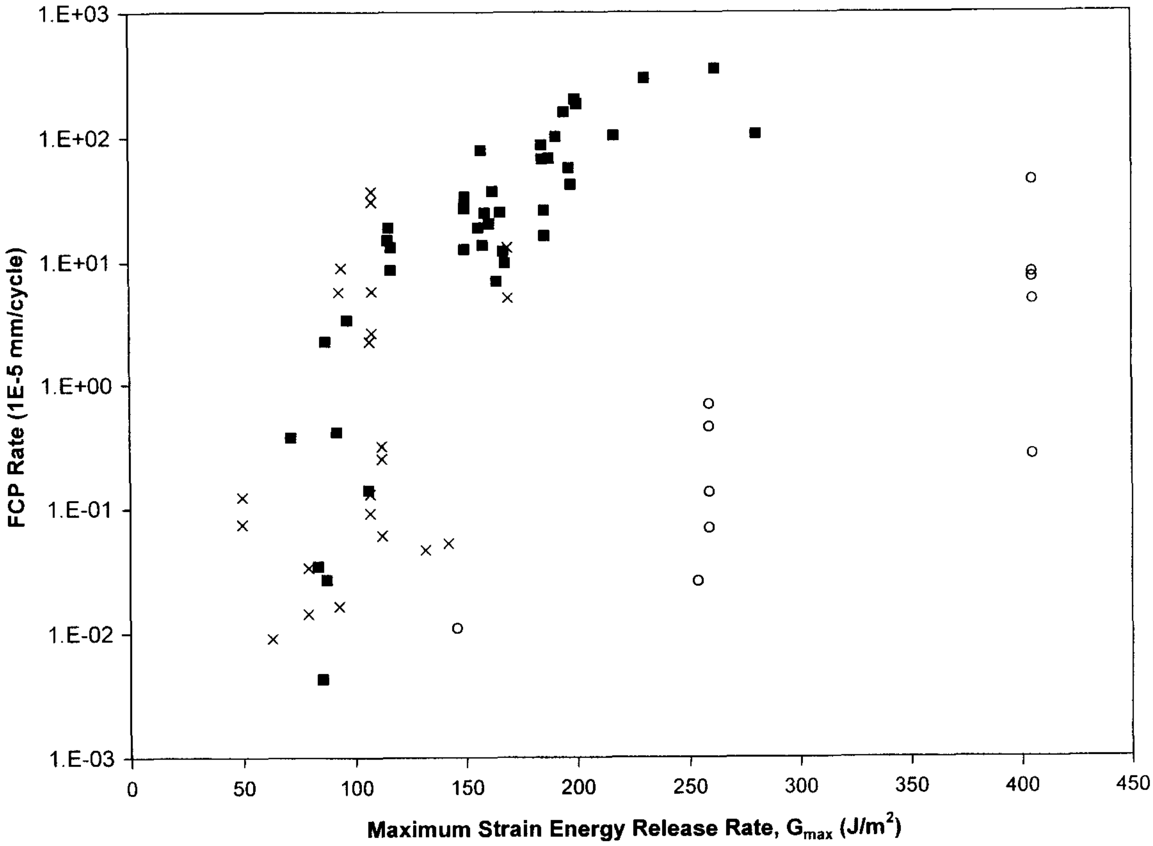

Figure 17 Fatigue crack propagation rate as a function of G_{max} for tests at three mode ratios; pure mode I (X), pure mode II (○) and mixed-mode I–II (■)

threshold $\%G_c$ values for modes I, I–II, and II, are respectively: 11, 9 and 19 for 10^{-7}mm/cycle, and 47, 19 and 39 for 10^{-5}mm/cycle. The data of *Figure 17*, shows that, in terms of G_{max}, the threshold for 10^{-7}mm/cycle is approximately 75J/m^2 for all mode ratios, and approximately 100J/m^2 for 10^{-5}mm/cycle for modes I and I–II. The second method of estimating the threshold energy release rate can be evaluated using the data of *Figure 11*. Here it is seen that both the mode I and mixed mode I–II initiation time of 10^6 cycles corresponds approximately to a G_{max} of 65J/m^2, in good agreement with the FCP result from *Figure 17*.

Note that in *Figure 13* there are a few data points at low $\%G_c$ that appear to lie on a steeper line, suggesting that they represent crack growth below the 'knee' of the fatigue curve. These points were included in the single overall regression, although leaving them out does not significantly affect the result.

Comparison to literature

Starting conditions. Murri and Martin[8] tested the effect of initial delamination on the mode I and mode II fatigue crack propagation thresholds of 24-ply glass/epoxy specimens. They used DCB (mode I) and ENF (mode II) specimens with Kapton inserts at the mid-plane to simulate initial delamination. Four insert thicknesses were used as different crack starting conditions as well as mode I and mode II precracks. They found that the precracks resulted in lower threshold values than the simulated delamination[8,9]. For the DCB specimens, generating the mode II precrack created microcracks ahead of the delamination front. They concluded that the coalescence of these microcracks accelerated the delamination growth. For the mode II (ENF) tests, lower G_{th} values were obtained with thinner inserts, while similar G_{th} values were obtained with mode I and mode II precracks.

Though the current adhesive joint system is not a composite laminate, it is interesting to compare the effect of a simulated debond with Murri and Martin's findings. In the present case, there was negligible difference in t_i for mode I crack initiation from a fast mode I precrack or from a Teflon insert. From these findings, it is postulated that G_{th} may be similar for both. The mode I precracks created microcracks, ahead of the macroscopic crack tip, however, unlike the effect of mode II precracks in Murri and Martin's study, these microcracks did not appear to affect crack initiation.

Fatigue crack initiation compared to quasi-static and creep crack initiation. Fatigue loading of joints is more damaging than creep and quasi-static loading of joints. In the present experiments, crack initiation was obtained at load levels as low as $17\%G_c$ ($\psi\sim60°$). Papini *et al.*[10] found that fillets of unequal adherend CLS joints ($\psi\sim60°$), made with the same adhesive system used in the present research and loaded quasistatically, initiated cracks at 55–65%G_c. After this, approximately 5mm of growth was required with increased loading to have a fully-developed failure zone at which point $G_{applied} = G_c$ and the crack grew catastrophically. Creep tests with the same adhesive system in a modified DCB loaded in mixed mode I–II at $\psi = 41°$ led to a recommended threshold value for creep loading of 62%G_c [5].

Effect of mode ratio. Mall and Yun[6] report on mode I and mixed-mode fatigue experiments with relatively ductile and brittle epoxy adhesives, concluding that the crack propagation trends are quite dependent on the adhesive. For example, with the more ductile adhesives (FM300 and EC3445), the total energy release rate proved to be the best correlating parameter, however, crack growth rates in a more brittle adhesive (FM400) were consistently higher under mixed mode-mode loading than under pure mode I loading at a given total energy release rate. These same differences and trends were also evident when the growth rate data were plotted as a function of the fraction of the quasi-static critical energy release rate, G/G_c. Comparison with the present data suggests that these different patterns of behaviour are not well predicted using the descriptors 'brittle' and 'ductile'. The present adhesive, Cybond 4523GB, is even more brittle than FM400 ($E = 8.0$ GPa, $G_{IC} = 200$mJ/m^2 compared with $E = 4.8$ GPa, $G_{IC} = 600$J/m^2 for FM400) yet shows similar crack growth rates for a given G_{max} under mixed-mode and mode I loading, and higher mixed-mode propagation rates for a given %G_c. In other words, Cybond 4523GB displays a trend like FM400 when propagation is plotted against %G_c, and a trend like the more ductile FM300 and EC3445 when propagation is plotted against G_{max}. Note that Mall and Yun[6] did not report data for pure mode II loading.

O'Brien[11] also concluded that G_T appeared to be the controlling parameter for debond initiation and propagation in tough structural adhesives, similar to the observations of Mall and Yun[6] for their relatively 'ductile' adhesives.

Brussat and Chiu[12] also found that da/dN was dependent on ψ and the total energy release rate. They tested CLS and contoured double cantilever beam (CDCB) specimens made of an aluminium alloy and a film epoxy adhesive. For a given value of G_I (or G), their mixed mode I–II data had a higher propagation rate than for mode I. This is in agreement with the results of Mall and Yun[6] for 'brittle' adhesives and the present results when plotted against %G_c, but inconsistent with the present data plotted versus G_{max}.

Everett Jr[13] found that G_I was the driving component for debonding of CLS joints consisting of a 14-ply laminate of unidirectional graphite/epoxy bonded to an aluminum alloy with a room temperature curing epoxy adhesive. However, only one mode ratio (55°) and one load level (or one G_T) were tested at a frequency of 9Hz and a load ratio (R) of 0.1. Imanaka *et al.*[14] observed that the torsional fatigue strength (shear) in butt joints is higher than under tensile fatigue, suggesting that mode I (peel) stresses are more damaging than mode II (shear) stresses, supporting Everett's findings, and in agreement with the present trend of mode II propagation data relative to that of the mode I data. However, this is unlike results seen by Mall *et al.*[15] for graphite fibre composites and Martin and Murri[9] for a tough thermoplastic matrix composite (AS4/PEEK) where mode II FCP rates were greater than those in mode I. It is evident that the effect of mode ratio on fatigue crack propagation is a function of the mechanical properties of the particular adhesive being tested.

Scatter. It is well known that a large amount of scatter complicates the interpretation of fatigue data for adhesive joints[16]. The FCP rates measured by Everett and Johnson[17] varied by a factor of 2 to 7. Joseph *et al.*[18] found that in aluminium DCB specimens bonded with FM-73 structural film adhesive, the FCP rates are varied up to a factor of 15. Greater scatter was observed for joints which failed adhesively instead of cohesively.

Conversely, Kinloch and Osiyemi[19] obtained very little scatter with a DCB joint consisting of fibre-composite adherends (epoxy-based unidirectional carbon-fibre material) bonded with an epoxy-film adhesive (FM73M). They maintained a displacement ratio of 0.5 and a frequency of 5Hz during testing. Data were collected over a range of G_{max} values, but for a given G_{max} value, only one FCP rate was presented except near G_{th}. Because of the data reliability, they were able to formulate a predictive fatigue life model.

In the present study, the greatest scatter in FCP rates was seen with the mode I DCB tests. For the specimens whose cracks did not arrest, there was a maximum factor of 37 difference in FCP rates at 70%P_f. At the other load ranges, the FCP rates varied by a factor of 5–13 for the DCB joints. A factor of approximately 5 was seen in the FCP rates measured with the mixed-mode CLS joints for the load ranges of 45% to 60% P_f. For the mode II tests conducted on ENF joints, the variation of the FCP rates was high, with a factor of 26 at 60%P_f and 10 at 75%P_f. One possible explanation for this scatter is the relatively large amount of mineral filler (approximately 50% by weight), and the presence of 1% by weight glass spacing beads. This paste adhesive is, therefore, much more heterogeneous than a film epoxy such as FM-73.

The steep FCP slopes indicate that adhesive joints bonded with Cybond 4523GB are very sensitive to small changes in loads. This, plus the large variability in FCP rates, makes it unreliable to design joints using finite life or crack growth calculations. It is, therefore, desirable to obtain energy release rate threshold values for design purposes, and to restrict operating loads so that no cyclic debonding occurs. Schmueser[20] reached the same conclusion based on fatigue tests with CLS joints consisting of mild steel adherends bonded with a one-part epoxy.

CONCLUSIONS

Adhesive joints comprised of a structural epoxy paste adhesive (Cybond 4523GB) were tested under fatigue loading over a range of loads, with several different starting conditions and under three mode ratios. The following conclusions can be drawn for this particular adhesive system:

(1) Joints made with this adhesive system, subject to cyclic loading, should be designed for zero crack growth based on fatigue threshold values. The variability of the crack propagation rates, and their extreme sensitivity to changes in G make finite-life design (design based on anticipated propagation rates) uncertain for adhesives of this type.

(2) Under mode I cyclic loading with the present adhesive system, a pre-existing fatigue crack will take approximately two to three times longer to begin growing under a new load range than will a fast mode I precrack. Negligible differences in initiation times under mode I loading were seen between fast mode I precracks and undamaged cracks fronts simulated by Teflon inserts.

(3) Under a typical mixed I–II loading, the initiation of crack growth occurred after approximately the same number of cycles regardless of the starting condition; i.e. undamaged fillet, fast mode-I precrack, and a pre-existing fatigue crack. The same was true under mode II conditions.

(4) For the adhesive system tested, the relative influence of the mode ratio depended on whether the rate of crack propagation was plotted versus G_{max} or $\%G_c$ (percentage of the quasi-static critical energy release rate at the particular mode ratio). When expressed as a function of $\%G_c$, debonding rates were greatest under mixed-mode conditions at a given $\%G_c$, and were indistinguishable under mode I and mode II loading. However, when expressed as a function of G_{max}, the propagation rates at a given G_{max} were the same under mixed-mode and mode I loading, and smaller under mode II loading. This means that the allowable loads for joints in fatigue will depend on the mode ratio; for mixed-mode joints it will be a smaller fraction of the quasi-static allowable load than for mode I or mode II joints.

(5) Threshold energy release rates (G_{max}) under mode I and mixed mode I-II loading were essentially the same, and were obtained equally from extrapolated crack propagation rates or crack initiation times.

(6) Fatigue loading significantly reduced the strain energy release rate required to initiate a crack compared to both creep and quasi-static loading.

ACKNOWLEDGEMENTS

We gratefully acknowledge the support of the Natural Sciences and Engineering Research Council of Canada, American Cyanamid, and the Manufacturing Research Corporation of Ontario.

REFERENCES

1 Fernlund, G. and Spelt, J.K. *Int. J. Adhesion and Adhesives* 1991, **11**, 213–220.
2 Fernlund, G., Papini, M., McCammond, D. and Spelt, J.K. *Compos. Sci. Technol.* 1994, **51**, 587–600.
3 Fernlund, G. and Spelt, J.K. *Compos. Sci. Technol.* 1994, **50**, 441–449.
4 Mall, S., Johnson, W.S. and Everett, R.A., Jr, in *Adhesive Joints: Their Formation, Characteristics and Testing*, ed. K.R. Mittal. Plenum Press, New York, 1984, pp. 639–658.
5 Plausinis, D. and Spelt, J.K. *Int J. Adhesion and Adhesives* 1995, **15**, 143–154.
6 Mall, S. and Yun, K.T. *J. Adhesion* 1987, **23**, 215–231.
7 Plausinis, D. and Spelt, J.K. *Int. J. Adhesion and Adhesives* 1995, **15**, 225–232.
8 Murri, G.B. and Martin, R.H. in *Composite Materials: Fatigue and Fracture*, Vol. 4, ASTM STP 1156, ed. W.W. Stinchcomb and N.E. Ashbaugh. American Society for Testing and Materials, Philadelphia, 1993, pp. 239–256.
9 Martin, R.H., Murri, G.B., in *Composite Materials: Testing and Design*, Vol. 9, ASTM STP 1059, ed. S.P. Garbo. American Society for Testing and Materials, Philadelphia, 1990, pp. 251-270.
10 Papini, M., Fernlund, G. and Spelt, J.K. *Compos. Sci. Technol.* 1994, **52**, 561–570.
11 O'Brien, T.K., Mixed-Mode Strain Energy Release Rate Effects on Edge Delamination of Composites, NASA TM-84592, National Aeronautics and Space Administration, Washington, D.C., Jan. 1983.
12 Brussat, T.R. and Chiu, S.T. *J. Engineering Materials and Technology* 1978, **100**, 39–45.
13 Everett, R.A., Jr, "The Role of Peel Stresses In Cyclic Debonding", *Adhesives Age*, May 1983, pp. 24–29.
14 Imanaka, M., Fukuchi, Y., Kishimtot, W., Okita, K., Nakayamma, H. and Nagai, H. *J. Engineering Materials and Technology* 1988, **110**, 350–354.
15 Mall, S., Yun, K.-T., and Kochhar, N.K. in *Composite Materials: Fatigue and Fracture*, Vol. 2, ASTM STP 1012, ed. Paul A. Lagace. American Society for Testing and Materials, Philadelphia, 1989, pp. 296–310.
16 Schijve, J. *Fatigue Fracture Engineering Mater. Struct.* 1994, **17**(4), 381–396.
17 Everett, R.A. and Johnson, W.S., in *Delamination and Debonding of Materials*, ASTM STP 876, ed. W.S. Johnson. American Society for Testing and Materials, Philadelphia, 1985, pp. 267–281.
18 Joseph, R., Bell, J.P., McEvilly, A.J. and Liang, J.L. *J. Adhesion* 1993, **41**, 169–187.
19 Kinloch, A.J. and Osiyemi, S.O. *J. Adhesion* 1993, **43**, 79–90.
20 Schmueser, D.W. *J. Adhesion* 1991, **36**, 1–23.